

THE NUCLEON'S VIRTUAL MESON CLOUD AND DEEP INELASTIC LEPTON SCATTERING

W. Koepf and L.L. Frankfurt*

School of Physics and Astronomy

Raymond and Beverly Sackler Faculty of Exact Sciences

Tel Aviv University, 69978 Ramat Aviv, Israel

M. Strikman[†]

Pennsylvania State University, University Park, PA 16802, USA

(July 4, 1995)

Abstract

We address the question whether the nucleon's antiquark sea can be attributed entirely to its virtual meson cloud and, in essence, whether there exists a smooth transition between hadronic and quark-gluon degrees of freedom. We take into account contributions from π and K mesons and compare with the nucleon's antiquark distributions which serve as a non-perturbative input to the QCD evolution equations. We elucidate the different behavior in the flavor singlet and non-singlet channels and study the dependence of our results on the scale Q^2 . The meson-nucleon cut-offs that we determine

*On leave of absence from the St. Petersburg Nuclear Physics Institute, Russia.

[†]Also St. Petersburg Nuclear Physics Institute, Russia.

give not only an indication on the size of the region within which quarks are confined in a nucleon, but we find that the scale of these form factors is closely related to the four-momentum transfer, Q^2 , where gluons are resolved by a high energy probe, and that large meson loop momenta, $|\mathbf{k}| \approx 0.8$ GeV, contribute significantly to the sea quark distributions. While the agreement of our calculations with data-based parametrizations is satisfactory and scale independent for the flavor breaking share of the nucleon's antiquark sea, the flavor singlet component is quite poorly described. This hints the importance of gluon degrees of freedom.

PACS number(s): 13.60.Hb, 13.75.Gx, 13.75.Jz

I. INTRODUCTION

Ever since the postulation of mesons by Yukawa in 1934, and the discovery of the pion in 1947, it has been clear that mesons play a crucial role in low-energy nuclear physics. The long-range part of the nucleon-nucleon interaction at low energies is clearly dominated by one-pion exchange, and direct evidence for the role of mesons in nucleon structure comes from the negative charge radius of the neutron which can be attributed to the virtual $n \rightarrow p\pi^-$ process. Furthermore, meson-exchange currents have proven to be essential for a quantitative description of many low-momentum-transfer processes, as, for instance, radiative neutron capture at threshold, near-threshold electro-disintegration of the deuteron, and the isovector magnetic form factors of nuclei. Also, a non-perturbative pionic cloud around the nucleon offers a straightforward explanation [1] of the $SU(2)$ flavor asymmetry of the proton's antiquark sea observed in the NMC experiment [2].

The fundamental role of pion clouds in nuclear physics is well explained in QCD as a consequence of the spontaneously broken chiral symmetry, and an interesting and important question is on the region of applicability of Chiral QCD Lagrangians, and at what distance scale this description will fail. It is the purpose of this work to investigate whether there exists a smooth transition between low-energy nuclear physics degrees of freedom, i.e., baryons and mesons, and a description in terms of quarks and gluons which is adequate for hard processes. In particular, we study whether the nucleon's antiquark distributions, as observed in inclusive, unpolarized, deep inelastic lepton and neutrino scattering, can be attributed entirely to its virtual meson cloud or if they should be described in terms of quarks and gluons. For this aim, we compare the contribution of the meson cloud with primary sea quark distributions which serve as a non-perturbative input to the QCD evolution equations.

In traditional nuclear physics, the crucial quantity which determines the strength of the pionic contribution to the nucleon's structure is the πNN form factor. In a quark model picture, the latter is intimately related to the confinement size of the quarks, and there is a long standing theoretical puzzle associated with it. The need for a sufficiently strong tensor

force to reproduce the D/S ratio and the quadrupole moment of the deuteron suggests a rather hard πNN vertex at small momentum transfers, and consequently most NN meson-exchange potentials which are fit to the rich body of NN phase shift data have a relatively high momentum-cut-off, with, for example, $\Lambda_{\pi NN} = 1.3$ GeV in monopole form for the Bonn potential [3].

On the contrary, hadronic models of baryons with meson clouds, like the Skyrmin, typically have a rather soft πNN form factor [4], in a quenched lattice QCD calculation a soft form factor was "measured" with a monopole mass of $\Lambda_{\pi NN} = 0.75 \pm 0.14$ GeV [5], and also in a recent analysis in the framework of QCD sum rules a soft monopole cut-off of $\Lambda_{\pi NN} \approx 0.8$ GeV was suggested [6]. In addition, there is further evidence for a fairly soft πNN vertex from other sources: arguments based on resolving the Goldberger-Treiman discrepancy [7] as well as the apparent charge dependence of the $pp\pi^0$ and $pn\pi^+$ couplings [8] both suggest a relatively soft πNN form factor with $\Lambda_{\pi NN} \approx 0.8$ GeV. Threshold pion production from pp scattering can best be reproduced by using a soft πNN vertex, with $\Lambda_{\pi NN} \approx 0.65$ GeV [9], and pion electro-production data on hydrogen also point towards a very soft πNN form factor [10]. Today, there exist efforts to reconcile the NN phase shift data with a soft πNN vertex. The inclusion of $\pi\pi$ interactions [11] as well as $\pi\rho$ scattering [12] allows one to avoid the need for hard form factors, and Haidenbauer et al. [13] presented a successful model where both one- and two-pion exchanges were included with soft πNN and $\pi N\Delta$ vertices.

Furthermore, a soft $\Lambda_{\pi NN}$ is preferable to avoid contradictions with data on the nucleon's antiquark distributions. Thomas [14] pointed out that deep inelastic scattering data on integrals over the momentum carried by sea quarks in the proton, i.e., sum rules, can be used to restrict the t -dependence of the πNN vertex. Frankfurt et al. [15] showed that to describe the steep decrease of the sea quark distributions with x the vertex cut-off, in a monopole parametrization, should be less than 0.5 GeV. Subsequently, sparked by experimental results of the NMC group [2] which suggested a violation of the Gottfried sum rule the analysis of this mechanism was focused on the $SU(2)$ breaking component of the quark sea [1,16–20],

and more mesons were included into the nucleon's virtual cloud [21–23].

In many early works in that realm solely integrated quantities, i.e., sum rules, were discussed [1,14,17], and in others either only the flavor breaking share of the nucleon's antiquark sea was considered [16,18–20] or the analysis was limited to certain combinations of the nucleon's sea quark distributions [15,23]. In Refs. [21,22], the nucleon's entire antiquark sea was attributed to its meson cloud at a scale of $Q^2 \approx 17 \text{ GeV}^2$ while using hard vertices which are almost consistent with the Bonn meson-exchange model. Their conjecture, however, is based predominantly on integrated quantities (sum rules), and the contribution of the mesonic cloud was multiplied with a wave function renormalization factor which is at variance with the standard nuclear physics definition of the πNN coupling constant [23], as will be clarified later. Besides, to describe the flavor asymmetry in the sea quark distributions specific assumptions on the quark distributions in the bare, recoiling baryons were needed.

Also in this work, we investigate the possibility to attribute the nucleon's full antiquark sea to its virtual mesonic cloud. However, we do not consider sum rules which contain contributions from the small x region where shadowing effects are important, but we study the x -dependence of the antiquark distributions, emphasizing especially the tails of the parton distribution functions which are most sensitive to the meson-nucleon form factors.

For the first time, the dependence of the parameters which characterize the underlying convolution picture, i.e., the cut-offs at the vertices, on the scale, Q^2 , where perturbative QCD evolution of the non-perturbative sea quark distributions starts is studied, and the qualitatively different behavior in the flavor singlet and non-singlet channels is elucidated. Also, we analyze which mesonic virtualities and loop momenta yield the dominant contributions in the respective convolution integrals, and, in essence, whether there exists a smooth transition between hadronic and quark-gluon degrees of freedom.

Recently, new improved fits of the nucleon's unpolarized parton distributions to a host of deep inelastic scattering data became available from Martin, Roberts and Stirling [24] as well as the CTEQ collaboration [25]. Using those, we update the analysis of the contribution of

the virtual meson cloud of the nucleon to its antiquark distributions, and separately adjust the πNN , KNY (where $Y \in \{\Lambda, \Sigma, \Sigma^*\}$) and $\pi N\Delta$ form factors to the flavor $SU(3)$ and $SU(2)$ breaking components of the nucleon's antiquark sea and to its strange quark content, following the framework presented, for instance, in Refs. [1,14,15,26].

In particular, we fit the various meson-nucleon vertices to the nucleon's antiquark distributions at different values of the four-momentum transfer, Q^2 , where the contamination from gluon splitting into $q\bar{q}$ pairs is not yet dominant. In addition to the major contribution arising from virtual pions, we also consider the kaonic cloud, with the corresponding coupling constants fixed by spin-flavor $SU(6)$ which holds much better for the coupling constants than it does for the masses, as has been observed in hyperon-nucleon scattering [27]. However, other mesons whose contributions are even more suppressed as due to their higher masses were not considered.

The form factors that we determine in this work are still significantly softer than what is used in most meson-exchange models of the NN interaction, and they indicate that the $\pi N\Delta$ vertex is considerably softer than the πNN vertex and that the cut-offs in the strange sector are harder than in the non-strange sectors. We analyze the relationship between the hardness of the meson-nucleon form factors and Q^2 , the scale where QCD evolution begins. While the agreement of our calculations with the data-based parametrizations is satisfactory and practically scale independent for the flavor breaking share of the nucleon's antiquark distributions, the corresponding flavor singlet component is quite poorly described in the convolution picture and it is contaminated with a sound scale dependence. The meson virtualities and loop momenta that are relevant in the deep inelastic process investigated here, $t \approx -0.4 \text{ GeV}^2$ and $|\mathbf{k}| \approx 0.8 \text{ GeV}$, are very different from those probed in low-energy nuclear physics phenomena, as, for instance, in the meson-exchange descriptions of the NN interaction where meson momenta of the order of the pion mass are dominant, and the validity of Chiral QCD Lagrangians in this regime is questionable. Actually, the analysis performed here hints that hard form factors at the meson-nucleon vertex may reflect the presence of a gluon cloud in the nucleon which cannot be resolved by a low energy probe,

and that there exists no smooth transition between hadronic and quark-gluon degrees of freedom.

The organization of this work is as follows. In Sec. II, we review the theoretical framework with which we attempt to connect the nucleon's sea quark distributions to its virtual meson cloud. In Sec. III, we present results of our fits to the flavor $SU(3)$ and $SU(2)$ breaking components of the nucleon's antiquark sea and to its strange quark content. We discuss the results of our calculations in Sec. IV, and summarize and conclude in Sec. V.

II. THE PION CLOUD AND THE NUCLEON'S STRUCTURE FUNCTIONS

It has been suggested by Sullivan [26] that in lepton scattering the virtual one-pion exchange may give a significant contribution to the nucleon's deep inelastic structure functions which scales in the Bjorken limit like the original process, and the generalization of that mechanism is depicted in Fig. 1.

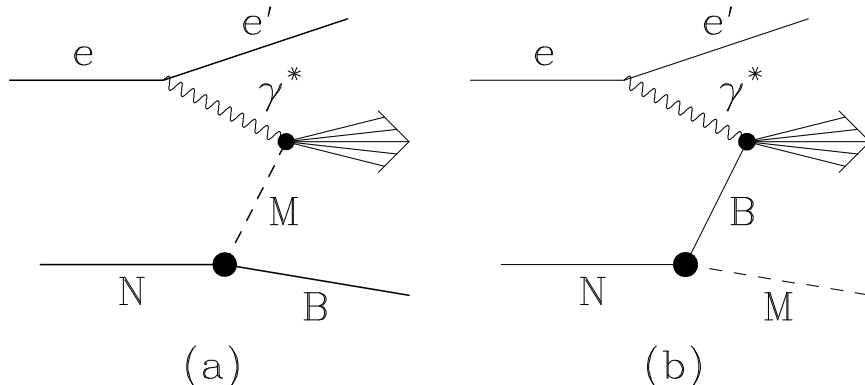


FIG. 1. The meson cloud contribution to the nucleon's structure functions in deep inelastic lepton scattering, where $B \in \{N, \Delta, \Lambda, \Sigma, \Sigma^*\}$ refers to an octet or a decuplet baryon accessible from the nucleon through emission of a meson, $M \in \{\pi, K\}$.

However, it is also common wisdom that, at large Q^2 , a significant fraction of the nucleon's antiquark sea originates from gluon splitting into $q\bar{q}$ pairs and not from the mesonic cloud. This perturbative process is approximately flavor symmetric and hence does not contribute to the flavor $SU(3)$,

$$x\bar{q}_8(x, Q^2) \equiv x \left[\bar{u}(x, Q^2) + \bar{d}(x, Q^2) - 2\bar{s}(x, Q^2) \right] , \quad (1)$$

and $SU(2)$,

$$x\bar{q}_3(x, Q^2) \equiv x \left[\bar{d}(x, Q^2) - \bar{u}(x, Q^2) \right] , \quad (2)$$

breaking components of the nucleon's antiquark distributions.

The direct meson cloud contribution of Fig. 1a can be written as a convolution of the virtual meson's antiquark distribution and its momentum dependence in the infinite momentum frame,

$$x\bar{q}_N(x, Q^2) = \sum_{M,B} \alpha_{MB}^q \int_x^1 dy f_{MB}(y) \frac{x}{y} \bar{q}_M\left(\frac{x}{y}, Q^2\right) , \quad (3)$$

where, in our investigation, the sum runs over $M \in \{\pi, K\}$ and $B \in \{N, \Delta, \Lambda, \Sigma, \Sigma^*\}$, and where the α_{MB}^q are spin-flavor $SU(6)$ Clebsch-Gordan factors. We assume the quark sea in the mesons to be flavor symmetric, and thus only the π and K *valence antiquark* distributions contribute to Eqs. (1) and (2). We neglect the slight difference between the latter, and take $x\bar{q}_\pi(x, Q^2)$ from fits to Drell-Yan pair production experiments. We also disregard contributions from mesons other than the π and the K which are strongly suppressed due to their higher masses as well as interference effects, as, for instance, between the π and the ρ . Actually, the latter vanish for the unpolarized distributions, to which we limit our discussions, because the corresponding trace over the baryon spinors and a pseudoscalar and a vector vertex is identically zero.

The virtual meson's light-cone distribution in the nucleon's cloud,

$$f_M(y) = \sum_B f_{MB}(y) , \quad (4)$$

which characterizes its probability of carrying a fraction y of the nucleon's momentum in the infinite momentum frame, can be expressed as

$$f_{MB}(y) = \frac{g_{MNB}^2}{16\pi^2} y \int_{-\infty}^{t_{min}} dt \frac{\mathcal{I}(t, m_N, m_B)}{(t - m_M^2)^2} F_{MNB}^2(t) , \quad (5)$$

where

$$\mathcal{I}(t, m_N, m_B) = \begin{cases} -t + (m_B - m_N)^2 & \text{for } B \in \mathbf{8} \\ \frac{((m_B + m_N)^2 - t)^2 ((m_B - m_N)^2 - t)}{12m_N^2 m_B^2} & \text{for } B \in \mathbf{10} , \end{cases} \quad (6)$$

for an intermediate, on-mass-shell octet or decuplet baryon, respectively, and where for the latter a Rarita-Schwinger spin vector was employed when evaluating the trace over the pseudoscalar vertices.

The integration in Eq. (5) is over the meson's virtuality, $t = k^2$, where $k = (m_N - \sqrt{m_B^2 + |\mathbf{k}|^2}, \mathbf{k})$ is its four-momentum, and the upper limit of the integration is determined purely by kinematics, with

$$t_{min} = m_N^2 y - \frac{m_B^2 y}{1 - y} . \quad (7)$$

Here, m_N , m_B and m_M are the nucleon mass, the mass of the intermediate baryon and the meson mass. For the pion-nucleon couplings we use the most recent values of the pseudoscalar coupling constants of $\frac{g_{\pi NN}}{\sqrt{3}} = 13.05$ [28] and $g_{\pi N \Delta} = 28.6$ [29], and the kaon-nucleon couplings are related to the latter using spin-flavor $SU(6)$ which agrees well with hyperon-nucleon scattering [27].

The only, a priori, unknown quantity in Eq. (5) is then the form factor, $F_{MNB}(t)$, which governs the emission of an off-mass-shell meson, and it is usually parametrized either in monopole, dipole or exponential (Gaussian) form, where

$$F_{MNB}(t) = \begin{cases} \frac{\Lambda_m^2 - m_M^2}{\Lambda_m^2 - t} & \text{monopole} \\ \left(\frac{\Lambda_d^2 - m_M^2}{\Lambda_d^2 - t} \right)^2 & \text{dipole} \\ e^{(t - m_M^2)/\Lambda_e^2} & \text{exponential} , \end{cases} \quad (8)$$

and where the cut-off masses can depend, in general, also on the meson-baryon channel under consideration. For our purposes, differences between the various forms given in Eq. (8) are not particularly important, and we will translate between the different cut-off parameters using the approximate relation given by Kumano [16],

$$\Lambda_m \approx 0.62\Lambda_d \approx 0.78\Lambda_e , \quad (9)$$

which is based on demanding an identical reduction of the various form factors of Eq. (8) to 40% of their pole values, i.e., $F_{MNB}^m(t_0) = F_{MNB}^d(t_0) = F_{MNB}^e(t_0) = 0.4$. With this, the form factors are compared at large virtualities, $t_0 \approx -\Lambda^2$. This is in contrast to the standard procedure of relating the different cut-off parameters by means of the slopes of the form factors at the meson poles, which, conversely, would lead to

$$\Lambda_m \approx \frac{\Lambda_d}{\sqrt{2}} \approx \Lambda_e, \quad (10)$$

and which is a good approximation for small virtualities. As the major contributions to the convolution integrals stem from fairly large mesonic virtualities of $t \approx -0.4 \text{ GeV}^2$, as will be discussed in Sect. IV.B, Eq. (9) is more appropriate in this realm than Eq. (10). Because for a monopole form factor the contribution to Eq. (5) from intermediate decuplet baryons is UV-divergent [15], we restrict ourselves to an exponential form in our actual calculations, which, in addition, yields the most satisfactory results.

We finally obtain for the flavor breaking components of the nucleon's antiquark distributions,

$$x \bar{q}_8(x, Q^2) = \int_x^1 dy [f_{\pi N}(y) + f_{\pi \Delta}(y) - 2f_K(y)] \frac{x}{y} \bar{q}_\pi\left(\frac{x}{y}, Q^2\right), \quad (11a)$$

$$x \bar{q}_3(x, Q^2) = \int_x^1 dy \left[\frac{2}{3}f_{\pi N}(y) - \frac{1}{3}f_{\pi \Delta}(y) \right] \frac{x}{y} \bar{q}_\pi\left(\frac{x}{y}, Q^2\right), \quad (11b)$$

with $f_{\pi N}(y)$ and $f_{\pi \Delta}(y)$ from Eq. (5), and $f_K(y)$ from Eq. (4). The fact, that the $N \rightarrow N\pi$ and $N \rightarrow \Delta\pi$ contributions add for the octet component in Eq. (11a) while they partially cancel for the triplet component in Eq. (11b) offers the possibility to separately determine $\Lambda_{\pi NN}$ and $\Lambda_{\pi N\Delta}$, as will be shown in the next section.

The theoretical framework presented in the above agrees with that employed in Refs. [1,26,14–17], except that we also consider kaonic loops and that we vary the form factors in the various meson-baryon channels independently. In Refs. [18,19,21,22,30], on the other hand, the Sullivan contribution, depicted in Fig. 1, was in addition multiplied with a wave function renormalization factor, $Z < 1$, where

$$Z = \left(1 + \sum_M n_M\right)^{-1} = \left(1 + \sum_M \int_0^1 dy f_M(y)\right)^{-1}. \quad (12)$$

This prescription is at variance with the fact that in coordinate space at large distances the meson-loop diagrams in Fig. 1 describe physical processes whose cross-sections involve physical, renormalized couplings. Note that this observation is used in nuclear physics to fix the πNN coupling constant.

In the underlying two-phase model, the physical nucleon, $|N\rangle$, is pictured as being part of the time a bare core, $|N_0\rangle$, and part of the time a baryon with one meson "in the air", $|BM\rangle$. In quantum field theory, bare, unrenormalized couplings, g_{MNB}^0 , should be used in the wave function of a physical particle when expressed in terms of its constituents, i.e.,

$$|N\rangle = \sqrt{Z'} \left(|N_0\rangle + \sum_M g_{MNB}^0 |BM\rangle \right). \quad (13)$$

Bare and renormalized couplings are, to lowest order, related via $g_{MNB} = \sqrt{Z'} g_{MNB}^0$, which allows us to rewrite Eq. (13) as [31]

$$|N\rangle = \sqrt{Z'} |N_0\rangle + \sum_M g_{MNB} |BM\rangle, \quad (14)$$

where the wave function renormalization factor,

$$Z' = 1 - \sum_M n_M = 1 - \sum_M \int_0^1 dy f_M(y), \quad (15)$$

now only affects the bare core, $|N_0\rangle$, and no longer the Sullivan contribution, $|BM\rangle$, as discussed in detail in Ref. [23]. This is the prescription which we follow, and it is consistent with the standard nuclear physics definition of the πNN coupling constant derived from the NN interaction at large distances.

Instead of the covariant formalism outlined here, in Refs. [19] and [23] "old-fashioned" time-ordered perturbation theory in the infinite momentum frame was used. The two diagrams in Fig. 1 are then treated on an equal footing, as the active particle and the spectator are both on their respective mass-shells. However, energy is not conserved at the meson-nucleon vertices, and the form factors, F_{MNB} , are unknown. In the covariant formalism, it

is thus more straightforward to compare the vertices – in the form of $F_{MNB}(t)$ of Eq. (8) – to standard nuclear physics quantities as, for instance, the vertex cut-offs of the Bonn potential.

III. THE NUCLEON'S ANTIQUARK SEA

A. The flavor non-singlet components:

After having outlined the theoretical framework, we present and discuss the results of our numerical calculations. In the first part of this section, we limit ourselves to the flavor breaking components, $x\bar{q}_8(x, Q^2)$ and $x\bar{q}_3(x, Q^2)$, defined in Eqs. (1) and (2). We determine the meson-nucleon cut-offs through the x -dependence of the various flavor non-singlet antiquark distributions in the nucleon by means of the convolution picture outlined in the above, and we compare results obtained at different scales, Q^2 , of 1, 2 and 4 GeV^2 . For the flavor non-singlet components $x\bar{q}_8(x, Q^2)$ and $x\bar{q}_3(x, Q^2)$ there is practically no contribution from gluon splitting into $q\bar{q}$ pairs, which is approximately flavor symmetric. Therefore, in this channel, the meson cloud picture has a good chance to describe the respective antiquark distributions, at least at a small scale of, for instance, $Q^2 = 1 \text{ GeV}^2$.

In Fig. 2, we show a comparison of our meson cloud calculations with various recent, empirical parton distribution functions, MRS(A') [24], CTEQ3M [25], GRV94(HO) [32], BM(A) [33] and MRS(D'_) [34], fit to the host of inclusive, unpolarized, deep inelastic lepton and neutrino scattering data. The mesonic contributions, as given in Eqs. (11a) and (11b), were obtained by evaluating the mesons' light-cone distributions in the nucleon's cloud with an exponential form factor using cut-off masses, $\Lambda_e = \Lambda_{\pi NN}^e = \Lambda_{K NY}^e = \Lambda_{\pi N \Delta}^e$, of 700, 800, 900 and 1000 MeV, and employing the NA24 pion structure function [35]. All curves shown correspond to a four-momentum transfer of $Q^2 = 1 \text{ GeV}^2$, and, where not directly available, the various PDFs were evolved by numerically [36] solving the non-singlet QCD evolution equations [37].

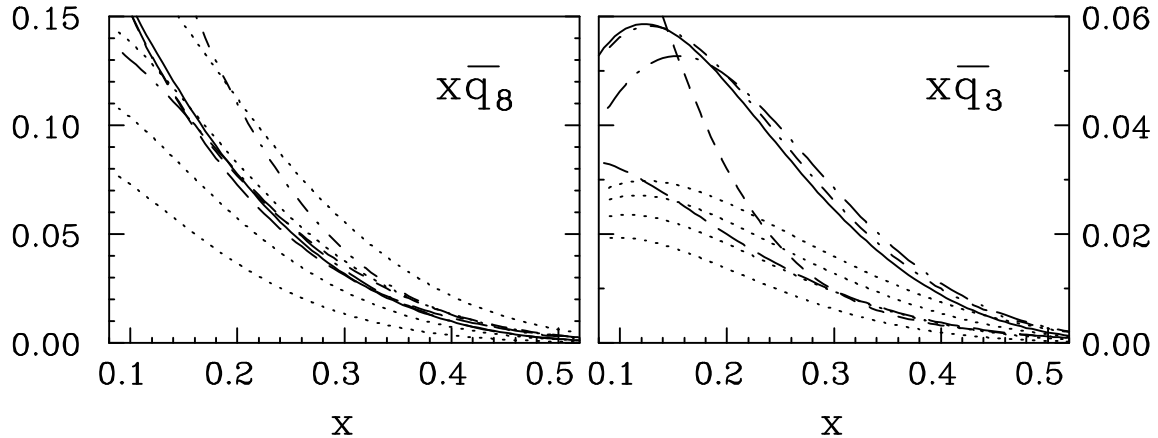


FIG. 2. The flavor breaking components of the nucleon's antiquark sea at $Q^2 = 1 \text{ GeV}^2$. The solid [dot-long-dashed, dot-short-dashed, short-dashed, long-dashed] curves correspond to the MRS(A') [CTEQ3M, GRV94(HO), BM(A), MRS(D'-)] PDFs, and the dotted lines refer to our meson cloud calculations using an exponential form factor and varying Λ_e between 700 and 1000 MeV.

As can be seen from Fig. 2, the various parton distribution functions (PDFs) agree well with each other in the $SU(3)$ channel, while there are significant discrepancies for the $SU(2)$ breaking component. Note that in a recent analysis of neutrino charm production it was observed that the nucleon's strange quark content is suppressed with respect to its non-strange sea by a factor of $\kappa = 0.48 \pm 0.06$ [38]. This is consistent with the two most recent PDFs of Refs. [24] and [25], where this reduction factor is $\kappa = 0.5$. Also, these two PDFs agree well with the x -dependence of the $(\bar{d} - \bar{u})$ asymmetry, as measured by the NA51 collaboration at CERN [39] and the CDF collaboration at the FNAL $p\bar{p}$ collider [40], while, for instance, in the BM(A) and MRS(D'-) distributions this asymmetry is concentrated at smaller x -values.

It is obvious from Fig. 2, that we can obtain a satisfactory fit to the $SU(3)$ breaking share of the nucleon's antiquark distribution, $x\bar{q}_8(x, Q^2)$, by varying the cut-off parameter in the aforementioned range. However, the agreement with the $SU(2)$ breaking component, $x\bar{q}_3(x, Q^2)$, this fit will yield, will be rather poor. In Table I, we nevertheless list the results of such a fit to the already shown and some additional parton distribution functions used

previously in this context. We employ two different pion structure functions, the NA10 parametrization from Ref. [41] and the NA24 parametrization from Ref. [35], fit to Drell-Yan data, and compare with the PDFs in the range of x -values of $0.2 \leq x \leq 0.5$. Again, where not directly available, the various PDFs were evolved down to the desired Q^2 by employing the LAG2NS code from Ref. [36]. The corresponding results are displayed in Fig. 3 for the MRS(A') and CTEQ3M parametrizations for values of the four-momentum transfer of 1 and 4 GeV².

PDF	Ref.	Year	$\Lambda_{\pi NN}^e = \Lambda_{KNY}^e = \Lambda_{\pi N\Delta}^e$ [MeV]					
			$Q^2 = 1 \text{ GeV}^2$		$Q^2 = 2 \text{ GeV}^2$		$Q^2 = 4 \text{ GeV}^2$	
			NA10	NA24	NA10	NA24	NA10	NA24
MRS(A')	[24]	(1995)	820	870	810	870	810	860
CTEQ3M	[25]	(1994)	830	880	810	870	810	860
GRV94(HO)	[32]	(1994)	900	940	890	950	890	940
BM(A)	[33]	(1993)	830	880	830	880	820	880
MRS(D' -)	[34]	(1993)	810	860	810	860	810	860
GRV(HO)	[42]	(1992)	800	850	790	840	790	840
MT(NS)	[43]	(1991)	700	730	690	730	690	730
HMRS(E)	[44]	(1990)	730	770	740	790	750	790
DFLM	[45]	(1988)	770	810	780	830	790	850
EHLQ(I)	[46]	(1984)	680	710	680	720	680	720

TABLE I. Results of a fit to the flavor $SU(3)$ breaking component of the nucleon's antiquark distribution at various Q^2 and for different PDFs. The range of x -values considered is $0.2 \leq x \leq 0.5$.

The MT [43], HMRS [44] and EHLQ [46] parametrizations, which would suggest even softer cut-offs, are today assumed to underestimate the nucleon's sea quark content. In the very recent GRV94 parametrization [32], on the other hand, it is assumed that the nucleon's strange quark sea vanishes at a very low renormalization scale, whereas $x\bar{s}$ is only suppressed

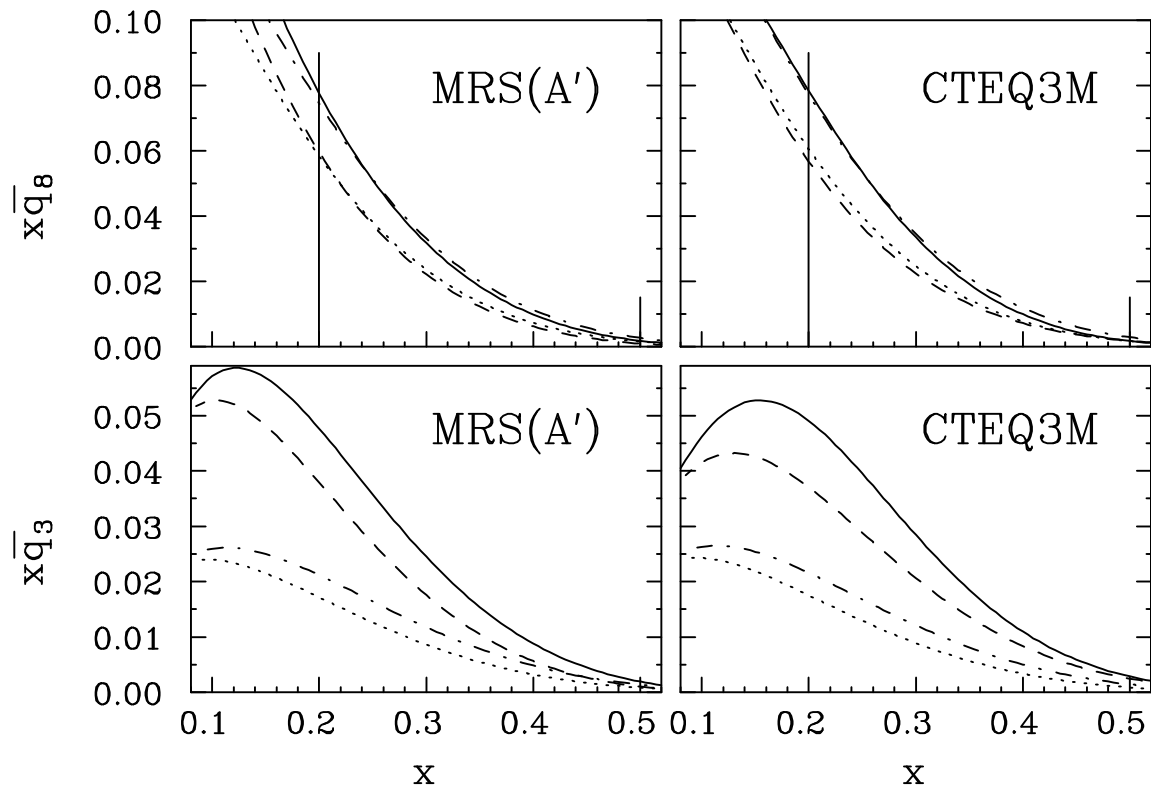


FIG. 3. The flavor breaking components of the nucleon's antiquark sea. The solid and dashed curves show the PDFs at $Q^2 = 1$ and 4 GeV^2 , and the dot-dashed and dotted lines refer to the corresponding meson cloud calculations using the NA24 pion structure function and employing Gaussian cut-offs of $\Lambda_e = 870$ and 880 MeV for the MRS(A') and CTEQ3M PDFs, respectively. The range of x -values considered in our fits is indicated through the vertical lines.

by a factor of $\kappa = 0.5$ in the PDFs of Refs. [24] and [25]. This manifests itself in a smaller strange quark sea, and hence a larger $x\bar{q}_8$, for the GRV94 parametrization, as can be seen in Fig. 2, and it leads to larger values for the cut-off parameter $\Lambda_{\pi NN}^e$ – but to softer form factors at the KNY vertex – that are necessary to describe this PDF. Furthermore, the $SU(3)$ breaking components of the MRS(A'), CTEQ3M, BM(A) and MRS(D'_) distributions agree quite well with each other, and the major uncertainties in our fit arise through the differences between the NA10 and NA24 pion structure functions.

Averaging over the MRS(A') and CTEQ3M parton distribution functions and the NA10 and NA24 pion structure functions at a scale of $Q^2 = 1 \text{ GeV}^2$ we find an exponential cut-off

mass of

$$\Lambda_e = \Lambda_{\pi NN}^e = \Lambda_{KNY}^e = \Lambda_{\pi N\Delta}^e \approx 850 \text{ MeV} . \quad (16)$$

This is significantly larger than the values¹ given by Melnitchouk and Thomas [23] (650 MeV), by Frankfurt et al. [15] (700 MeV), by Thomas [14] (700 MeV), and by Kumano [16] (750 MeV), where the now outdated MT [43], HMRS [44], DFLM [45], EHLQ [46], DO [47] or FF [48] parton distribution functions were used. It approximately agrees with the result of Melnitchouk et al. [18] (800 MeV), yet it is smaller than the values obtained by the Jülich group [21,22] (950 MeV) and by Signal et al. [17] (1000 MeV). The reason for the latter discrepancies is, firstly, that in Refs. [21,22] an additional renormalization of the Sullivan process was used which diminishes the mesonic contribution and hence leads to larger cut-offs and, on the other hand, that in Ref. [17] the $N \rightarrow \Delta\pi$ process was treated non-relativistically.

As can be seen from Fig. 3, our meson cloud calculations reasonably describe the $SU(3)$ breaking share of the nucleon's antiquark sea at the scale where the vertices were originally fit, i.e., at $Q^2 = 1 \text{ GeV}^2$. However, also at a scale of $Q^2 = 4 \text{ GeV}^2$, our calculations match the PDFs in that channel quite well. This suggests that for this component the perturbative evolution of the parton distributions in the nucleon as well as the pion by means of the non-singlet QCD evolution equations is compatible with the convolution of the latter distributions.

B. The nucleon's full antiquark sea:

It is obvious from Fig. 3 that our description of the flavor $SU(2)$ breaking component, $x\bar{q}_3(x, Q^2)$, is very poor, with the meson cloud calculations underestimating the data by about a factor of 2. We could cure this discrepancy, while preserving the good agreement

¹The results of the various calculations were translated into exponential form employing Eq. (9).

in the $SU(3)$ channel, by allowing the πNN , KNY and $\pi N\Delta$ vertices to be different, as is evident from Eqs. (11a) and (11b). In the following we thus vary the cut-offs in the octet and decuplet channel and in the strange and non-strange sectors separately. In essence, we fit Λ_{KNY}^e to the nucleon's strange quark content, $x\bar{s}(x, Q^2)$, and we then adjust $\Lambda_{\pi NN}^e$ and $\Lambda_{\pi N\Delta}^e$ to get an optimal description of the $SU(3)$ and $SU(2)$ flavor breaking components of the nucleon's antiquark sea, $x\bar{q}_8(x, Q^2)$ and $x\bar{q}_3(x, Q^2)$.

As the strange sea, $x\bar{s}(x, Q^2)$, contains a significant flavor singlet component, we are now *forced* to evaluate the PDFs at a small value of the four-momentum transfer where the contamination from gluon splitting into $q\bar{q}$ pairs is not yet dominant and where a comparison of hadronic and quark-gluon degrees of freedom might still be possible. In particular, we choose to work at a scale of $Q^2 = 1 \text{ GeV}^2$ – but we will also show results for larger Q^2 – and we consider x -values in the range of $0.3 \leq x \leq 0.5$. The results of such fits to the two most recent PDFs of Refs. [24] and [25] are listed in Table II. As the MRS(A') parametrization of Ref. [24] is not yet available at such low Q^2 , we restrict ourselves from now on to the very similar MRS(A) [49] parton distribution function. Furthermore, in the singlet channel also the meson's *sea quark* distributions contribute, however, at quite small x -values only.

PDF	$Q^2 \text{ [GeV}^2\text{]}$	$\Lambda_{\pi NN}^e \text{ [MeV]}$		$\Lambda_{\pi N\Delta}^e \text{ [MeV]}$		$\Lambda_{KNY}^e \text{ [MeV]}$	
		NA10	NA24	NA10	NA24	NA10	NA24
MRS(A) [49]	1	960	1010	780	790	1150	1180
	2	970	1030	800	820	1180	1220
	4	970	1030	840	860	1210	1250
CTEQ3M [25]	1	990	1050	810	810	1180	1210
	2	1010	1070	820	840	1220	1260
	4	1010	1080	860	870	1250	1290

TABLE II. Results of a fit to $x\bar{s}(x, Q^2)$, $x\bar{q}_8(x, Q^2)$ and $x\bar{q}_3(x, Q^2)$ of the nucleon at various scales, Q^2 , of 1, 2 and 4 GeV^2 . The range of x -values under consideration is $0.3 \leq x \leq 0.5$.

Again averaging over the MRS(A) and CTEQ3M parton distributions and the NA10 and NA24 pion structure functions we find exponential cut-offs of

$$\Lambda_{\pi NN}^e \approx 1000 \text{ MeV} , \quad (17a)$$

$$\Lambda_{\pi N\Delta}^e \approx 800 \text{ MeV} , \quad (17b)$$

$$\Lambda_{KNY}^e \approx 1180 \text{ MeV} , \quad (17c)$$

in the various relevant meson-baryon sectors at a scale of $Q^2 = 1 \text{ GeV}^2$. The corresponding antiquark distributions are depicted in Fig. 4 for values of the four-momentum transfer of 1 and 4 GeV^2 . Also shown are a few data points for $x\bar{s}(x, Q^2)$ as given by the CCFR collaboration [38].

As can be seen from Fig. 4, allowing the πNN and $\pi N\Delta$ vertices to be different significantly improves the quality of our fits to the $SU(2)$ flavor breaking component, $x\bar{q}_3(x, Q^2)$. Also, the agreement in both flavor breaking channels, $x\bar{q}_8(x, Q^2)$ and $x\bar{q}_3(x, Q^2)$, extends to smaller x -values than those actually considered in our fits, and it remains satisfactory when the four-momentum transfer is increased. This shows that the meson cloud picture put forward in this work may yield a satisfactory description of the nucleon's *flavor non-singlet* antiquark distributions down to x -values of $x \gtrsim 0.2$. Also, the perturbative evolution of the partonic distributions in the nucleon as well as the pion seems to be compatible with the convolution of the latter quantities in the non-singlet channels.

The situation is very different for the *flavor singlet* component. Due to the mixing with gluonic degrees of freedom, most notably through gluon splitting into $q\bar{q}$ pairs, we only find reasonable agreement with the tails of the $x\bar{s}$ and $x\bar{q}_0 \equiv x[\bar{u} + \bar{d} + \bar{s}]$ PDFs in the region of $x \gtrsim 0.3$. In addition, neglected shadowing effects tend to further decrease the cross section of lepton scattering from the MB component of the nucleon's wave function at small x . Furthermore, for $x\bar{s}$ and $x\bar{q}_0$ the deviations between our meson cloud calculations and the data-based parametrizations grow rapidly with increasing Q^2 , as can also be seen from Fig. 4. This indicates that, in the singlet channel, the evolution of the parton distribution functions is incompatible with the meson cloud convolution picture investigated here. This

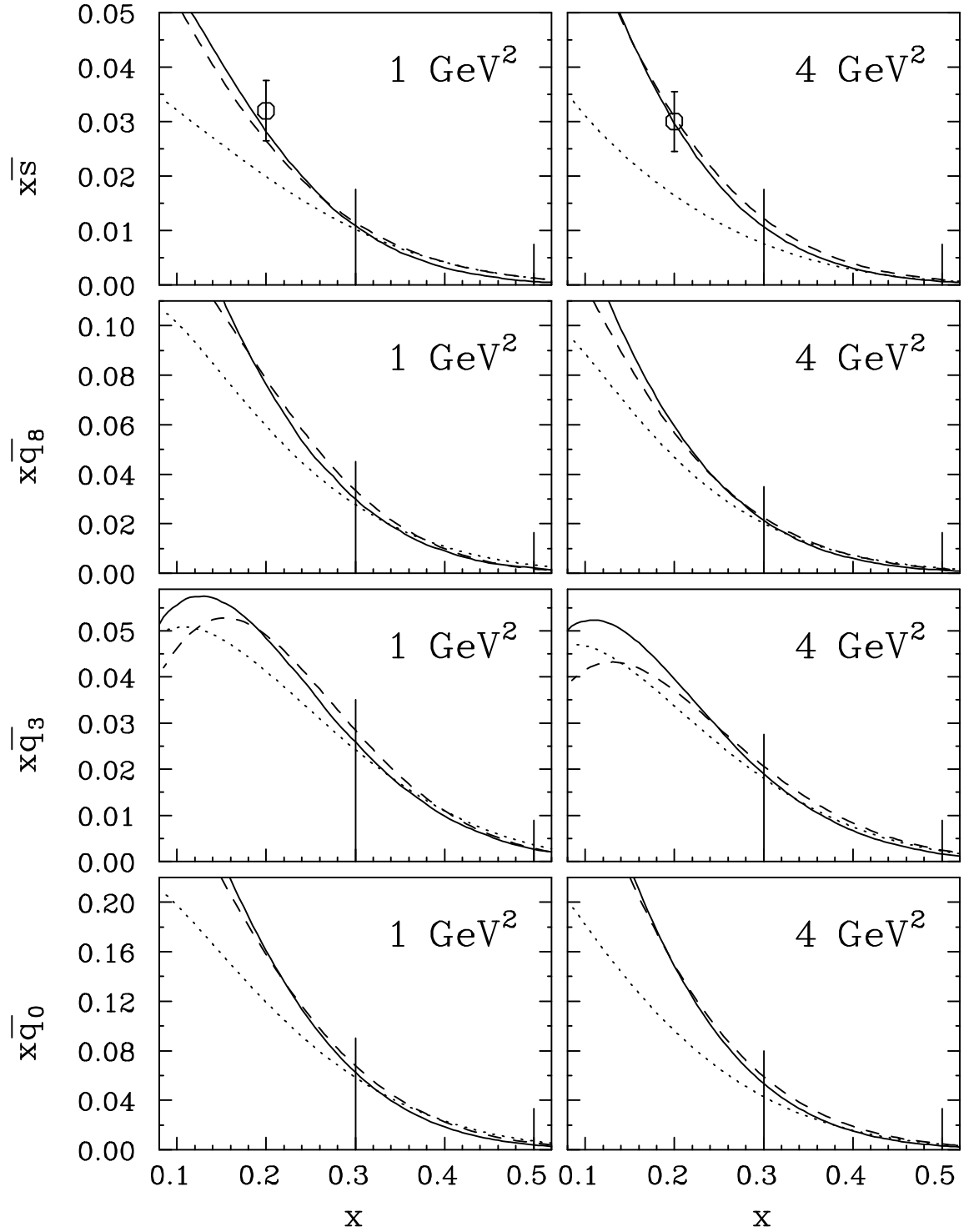


FIG. 4. The various components of the nucleon's antiquark sea. The solid and dashed curves show the MRS(A) and CTEQ3M PDFs, and the dotted lines refer to our meson cloud calculations using the NA24 pion structure function and the cut-offs $\Lambda_{\pi NN}^e = 1030$ MeV, $\Lambda_{\pi N\Delta}^e = 800$ MeV and $\Lambda_{KNY}^e = 1200$ MeV that were adjusted at a scale of $Q^2 = 1$ GeV².

stresses the importance of gluonic degrees of freedom in the flavor singlet channel, and it shows that the virtual meson cloud alone is not able to yield the nucleon's entire antiquark sea, even at a low scale of $Q^2 = 1 \text{ GeV}^2$.

IV. DISCUSSION

A. The meson-nucleon vertices:

The vertices that were determined in this work are still significantly softer than what is used in most meson-exchange models of the NN interaction or in evaluations of corresponding meson-exchange currents.² If we translate the $\Lambda_{\pi NN}^e$ of Eq. (17a) into a monopole cut-off using the approximate relation of Eq. (9)³ we find a value of $\Lambda_{\pi NN}^m \approx 800 \text{ MeV}$. This is much smaller than the respective quantity, $\Lambda_{\pi NN} = 1.3 \text{ GeV}$, employed in the framework of the Bonn potential [3], or the $\Lambda_{\pi NN} = 1.2 \text{ GeV}$ used in the evaluation of respective meson-exchange currents [50]. On the other hand, the $\Lambda_{\pi NN}^e$ of Eq. (17a) is not too far from the exponential cut-off used in the corresponding channel in the Nijmegen potential [51], $\Lambda_{PV} = 1195 \text{ MeV}$, or the Gaussian cut-off parameter employed by van Kolck et al. [52], $\Lambda \approx 1100 \text{ MeV}$, in their evaluation of nuclear forces from a Chiral Lagrangian.

In Ref. [53] kaon loop contributions to low-energy strange quark matrix elements, which will eventually be measured at CEBAF [54], were modelled employing the vertices from the Bonn YN potential [27]. Note that the corresponding KNY cut-offs are significantly harder

²In most MEC calculations the one-pion exchange is treated with point-like vertices combined with a hard-core short-distance cut-off in coordinate space, and, at this point, it is unclear whether this is consonant with our findings.

³We emphasize again that the contribution from decuplet baryons diverges when a monopole form factor is used, and that, hence, Eq. (9) is only applied in a qualitative manner in order to be able to compare with other works.

than that of Eq. (17c), which, in turn, has been determined directly from the strange quark distribution in the nucleon. Thus, if alternatively the quantity of Eq. (17c) would be used in their analysis the respective strangeness matrix elements would be strongly reduced, most likely down to the point where they could no longer be observed at CEBAF.

The cut-offs in Eqs. (17a) and (17b) indicate that the $\pi N\Delta$ vertex is considerably softer than the πNN vertex.⁴ This is in qualitative agreement with the faster fall-off of the electromagnetic $p \rightarrow \Delta$ transition form factor relative to the nucleon's elastic e.m. form factor as observed in exclusive resonance electron scattering [55]. Only in a pure $SU(6)$ model, where the quarks' spatial wave functions in the nucleon as well as the Δ are all identical $s_{1/2}$ states, are the form factors governing the processes $N \rightarrow \pi N$ and $N \rightarrow \pi\Delta$ necessarily the same. Already the one-gluon-exchange color-magnetic hyperfine interaction breaks that symmetry, and introduces a small $L = 2$ contribution into the Δ ground state [56]. There is experimental evidence for that admixture – and hence the breaking of the naïve $SU(6)$ symmetry – through the non-vanishing E2/M1 electromagnetic transition ratio observed in photoproduction data [29].

B. Structure of the nucleon:

Using a relation given by Thomas [14], the $\Lambda_{\pi NN}^e$ of Eq. (17a) can be converted into a MIT bag radius of $R \approx 0.60$ fm. This is somewhat smaller than what is usually cited in the literature [57] ($R \approx 1$ fm) when the nucleon's standard low-energy observables, as, for instance, its charge radius and magnetic moment, are described in the framework of that model. However, it agrees with the value favored by the Adelaide group [58] for the evaluation of the nucleon's deep inelastic structure functions from the MIT bag model. Our results, therefore, indicate a characteristic confinement radius of the quarks in a nucleon

⁴It was also mentioned in Ref. [21] that better agreement with the NMC data could be achieved in their meson cloud calculation if the $\pi N\Delta$ vertex would be softer than the πNN vertex.

of about 0.6 fm at a scale of $Q^2 \approx 1 \text{ GeV}^2$. Note, however, that the pion cloud yields a significant contribution to the nucleon's charge radius, i.e., $\langle r_c^2 \rangle = \langle r_q^2 \rangle + \langle r_\pi^2 \rangle$, and there is thus no contradiction between the result given here and the proton's experimental charge radius of 0.86 fm [59].

Furthermore, the perturbative two-phase picture of the nucleon, that was applied in this investigation, only makes sense if the mesonic component is just a perturbation, i.e., if the vertices are not too hard. Otherwise, higher-order diagrams with more than one pion present grow important, and the convergency of the whole approach becomes questionable. A quantitative measure of that is, for instance, the "number of mesons in the air",

$$n_M = \int_0^1 dy f_M(y) , \quad (18)$$

which is $n_\pi = 0.66$ and $n_K = 0.10$ for the cut-offs of Eqs. (17a) to (17c). Those values are already quite close to this limit of applicability of models of that type.

In Fig. 5, we visualize the dominant contributions to the convolution integrals of Eqs. (11a) and (11b). In particular, it is analyzed which region in the space spanned by the mesons' light-cone momentum fraction y , its virtuality t as well as the loop momentum $|\mathbf{k}|$ yields the largest share to $x\bar{q}_s(x, Q^2)$ for a typical x -value of $x = 0.3$ and for the case of the $N \rightarrow N\pi$ sub-process. We used a Gaussian cut-off of $\Lambda_{\pi NN}^e = 1030 \text{ MeV}$ and employed the NA24 pion structure function at a scale of $Q^2 = 1 \text{ GeV}^2$.

Fig. 5 shows that, for $x = 0.3$, the most relevant light-cone momentum fraction is the region $0.3 \leq y \leq 0.5$, which contributes 70% to the integral. Typically, the mesons in the loop are also highly virtual, with the areas $0.2 \text{ GeV}^2 \leq -t \leq 0.6 \text{ GeV}^2$, $0.6 \text{ GeV}^2 \leq -t \leq 1.0 \text{ GeV}^2$ and $-t \geq 1.0 \text{ GeV}^2$ yielding 45%, 30% and 20%, respectively. And, in contrast to low-energy nuclear physics phenomena where meson momenta around the pion mass are probed, the relevant loop momenta are here of the order of $|\mathbf{k}| \approx 0.8 \text{ GeV}$. In detail, the region of $|\mathbf{k}| \leq 0.5 \text{ GeV}$, which is most important in NN meson-exchange potentials, contributes only 15% to the deep inelastic process considered here. The dominant contributions, on the other hand, stem from the areas $0.5 \text{ GeV} \leq |\mathbf{k}| \leq 1.0 \text{ GeV}$ and

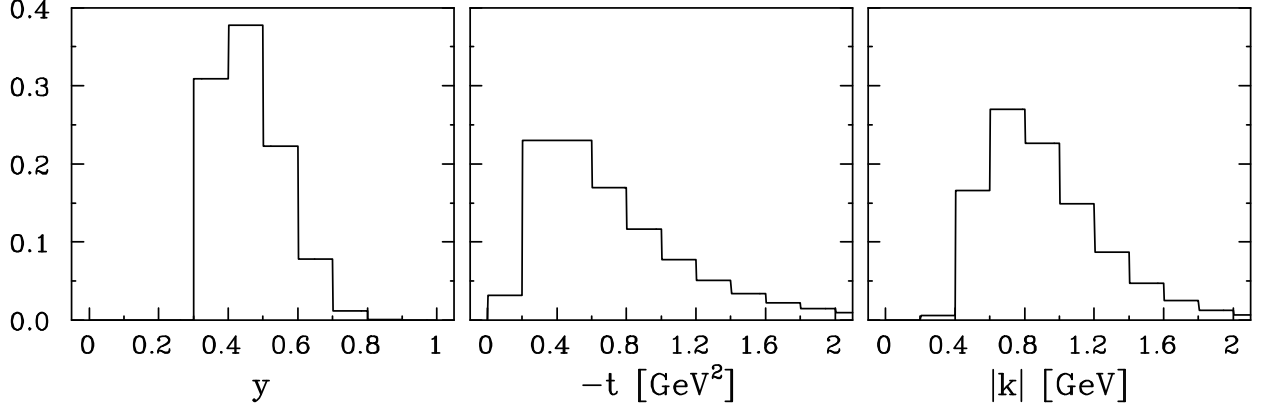


FIG. 5. The different relative contributions to the convolution integral of Eq. (11a) for the $N \rightarrow N\pi$ process from the various regions in the space spanned by the quantities y , t and $|\mathbf{k}|$, and for a typical x -value of $x = 0.3$.

$|\mathbf{k}| \geq 1.0$ GeV, which yield 50% and 30%, respectively. This indicates i) that a comparison of the cut-offs that we determine here with the corresponding quantities used in low-energy nuclear physics has to be looked upon with some caution, and ii) that the very idea of using meson clouds at such virtualities seems quite doubtful.

C. Gottfried sum rule:

If we evaluate the meson cloud contribution to the Gottfried sum rule,

$$S_G \equiv \frac{1}{3} - \frac{2}{3}\Delta_G \equiv \int_0^1 dx \frac{F_2^{\mu p}(x, Q^2) - F_2^{\mu n}(x, Q^2)}{x}, \quad (19a)$$

$$\equiv \frac{1}{3} \int_0^1 dx [u(x, Q^2) + \bar{u}(x, Q^2) - d(x, Q^2) - \bar{d}(x, Q^2)], \quad (19b)$$

$$= \frac{1}{3} + \frac{2}{3} \int_0^1 dx [\bar{u}(x, Q^2) - \bar{d}(x, Q^2)], \quad (19c)$$

with the vertices of Eqs. (17a) to (17c), we find a value of $\Delta_G = 0.17$ at $Q^2 = 4$ GeV². This agrees, within the error-bars, with the quantity given by the NMC collaboration of $\Delta_G^{exp} = 0.148 \pm 0.039$ [2]. Note that the direct meson cloud diagram, depicted in Fig. 1a, yields no contribution to Eq. (19b) due to G parity. It has been argued, for instance in Ref. [17], that the entire effect is thus due to the recoil baryon being struck by the incoming

meson, i.e., the diagram shown in Fig. 1b. However, conversely, only the direct meson cloud diagram of Fig. 1a contributes to Eq. (19c). The obvious solution to this paradox [22] is that Eqs. (19b) and (19c) are related through the normalization requirements for the valence quark distributions,

$$\int_0^1 dx [u(x, Q^2) - \bar{u}(x, Q^2)] = 2 , \quad (20a)$$

$$\int_0^1 dx [d(x, Q^2) - \bar{d}(x, Q^2)] = 1 , \quad (20b)$$

and the distinction between the direct mesonic and the recoil diagram is thus artificial, at least for the meson cloud contribution to the violation of the Gottfried sum rule.

It is common wisdom that, at small x and high energies, the dependence of the parton distributions on the invariant mass squared, W^2 , is governed by the exchange of the leading Regge pole in the t -channel of the elastic amplitude, which for the $SU(2)$ flavor breaking share of the nucleon's antiquark distribution leads to

$$x[\bar{d}(x, Q^2) - \bar{u}(x, Q^2)] \Big|_{x < 0.05} = c_3 x^{1-\alpha(A_2)} , \quad (21)$$

where $\alpha(A_2) \approx 0.4$ for the A_2 -meson's Reggeon that is relevant in this channel. In Ref. [60] it was argued that due to nuclear shadowing in the deuteron the cross section ratio F_{2n}/F_{2p} which was measured by the NMC collaboration [61] has to be modified at small x , and that hence $\bar{d}(x)/\bar{u}(x) > 1$ at $x = 0.007$. This indicates that the constant c_3 in Eq. (21) is larger than that assumed in the current parametrizations, and it was shown in Ref. [60] that the deviation of the Gottfried integral from $1/3$ observed by the NMC collaboration – which, in addition, should also be somewhat bigger than the value Δ_G^{exp} given in Ref. [2] again due to nuclear shadowing effects in the deuteron – can already be saturated by the region $0 < x < 0.02$ in the integral in Eq. (19c).

This suggests a reduction of the quantity $x(\bar{d} - \bar{u})$ at moderate x , as was originally assumed, for instance, in the MRS(D'_) PDF, and it would lead to a decrease of $\Lambda_{\pi NN}^e$ of Eq. (17a) and to an increase in $\Lambda_{\pi N\Delta}^e$ of Eq. (17b) in the realm of the meson cloud picture. Note, also, that only about 30% of the integral in Eq. (19c) stems from the area of $x > 0.1$,

where the meson cloud picture is at least somehow applicable, and the dominant contribution to Δ_G comes from the small- x region. This underlines our claim that, in this context, it is more appropriate to study the tails of the antiquark distributions than to solely concentrate on sum rules. There is an approved experiment at Fermilab, E866, which will measure the quantity $x(\bar{d} - \bar{u})$ over the whole relevant kinematic region and which will settle this issue [62].

D. Scale dependence and small x physics:

As already mentioned in the last section, the description of the *flavor non-singlet* share of the nucleon's antiquark distributions is quite satisfactory for x -values larger than about 0.2, and the quality of the agreement of our meson cloud calculations with the data-based PDFs is independent of the scale Q^2 . This indicates that the evolution of the partonic distributions in the framework of perturbative QCD and the convolution picture are compatible with each other, at least in the non-singlet channels.

The *flavor singlet* component, on the other hand, is quite poorly approximated through the mesonic cloud, even at a small scale of $Q^2 = 1 \text{ GeV}^2$. We are, in fact, only able to attribute the tails of the $x\bar{q}_0$ and $x\bar{s}$ distributions – the area of $x \gtrsim 0.3$ – to the nucleon's virtual meson cloud, and the deviations from the data-based parametrizations grow rapidly with increasing Q^2 . This indicates that, in the singlet channel, other degrees of freedom, most notably gluon splitting into $q\bar{q}$ pairs, are relevant, even at moderate x and small values of the four-momentum transfer.

The scale dependence of our results is analyzed in greater detail in Fig. 6, which depicts the πNN , $\pi N\Delta$ and KNY vertices that were determined in Sect. III.B (see Table II) from fits to the tails of the nucleon's entire antiquark sea at different values of the four-momentum transfer.

As can be seen from Fig. 6, the parameter Λ_{KNY}^e that is determined from $x\bar{s}(x, Q^2)$ which, in turn, is mostly flavor singlet shows a very strong scale dependence, and $\Lambda_{\pi NN}^e$ which is

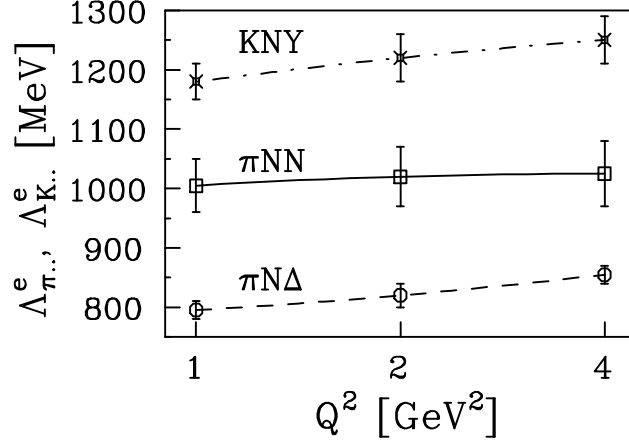


FIG. 6. The cut-off parameters $\Lambda_{\pi NN}^e$, $\Lambda_{\pi N\Delta}^e$ and Λ_{KNY}^e adjusted to fit the nucleon's antiquark distributions as functions of the scale, Q^2 , at which this fit is performed.

fixed through the flavor non-singlet distributions $x\bar{q}_8(x, Q^2)$ and $x\bar{q}_3(x, Q^2)$ hardly changes with Q^2 . This substantiates what has been discussed in the above about the qualitatively different behavior in the flavor singlet and non-singlet channels. The variations of $\Lambda_{\pi N\Delta}^e$ with Q^2 , on the other hand, are induced via the interplay of Eqs. (11a) and (11b) through the scale dependence of the KNY vertex which contributes not only to $x\bar{s}(x, Q^2)$ but also to the flavor non-singlet distribution $x\bar{q}_8(x, Q^2)$.

The strong Q^2 dependence of the KNY vertex signals a correlation between the presence of gluonic degrees of freedom at low Q^2 and contributions from the nucleon's virtual kaon cloud. At this point, both processes are indistinguishable, and the Λ_{KNY}^e given here has to be understood as an *upper bound*. As, in turn, a softer KNY vertex would lead also to a softer πNN vertex, as can be inferred from Eq. (11a), the values for $\Lambda_{\pi NN}^e$ listed in this work are actually *upper bounds* on that quantity. Thus, the scenario presented here has to be viewed as an extreme case. This conjecture is further supported by the fact that the meson cloud can only describe the tail of the flavor singlet antiquark distribution, while the mismatch at $x \lesssim 0.3$ is probably due to gluon splitting into $q\bar{q}$ pairs, and there are no stringent reasons why the influence of gluonic degrees of freedom should be limited to the aforementioned small- x range only.

This suggests that a smooth transition between the low-energy nuclear physics degrees

of freedom, i.e., baryons and mesons, and a description in terms of quarks and gluons which is adequate for hard processes does not seem to exist. It has been clearly shown in this work that, even at a small Q^2 , it is *not* possible to attribute the entire sea quark distributions in the nucleon to its mesonic cloud.⁵ Firstly, the meson-nucleon vertices which are necessary to describe the *flavor breaking* share of the nucleon's antiquark distributions in the meson cloud picture outlined here are significantly different from the respective quantities used in low-energy nuclear physics, as, for instance, the cut-offs employed in the Bonn potential. And, furthermore, even when freely adjusting the respective form factors, a satisfactory description of the *flavor singlet* component of the nucleon's antiquark sea is not possible. Not only are there large discrepancies already for x -values smaller than about 0.3, but also the perturbative evolution of the singlet component to higher values of the four-momentum transfer by means of the QCD evolution equations is incompatible with the meson cloud convolution picture. This shows that gluon degrees of freedom play an important role in the structure of the nucleon, even at a scale of $Q^2 = 1 \text{ GeV}^2$.

At small x and high energies the virtual photon converts into a hadronic $q\bar{q}$ state at a distance

$$l \approx \frac{1}{2m_N x} \quad (22)$$

in the target rest frame. If this coherence length is larger than the dimension of the target,

$$l \gtrsim 2 \langle r_T \rangle , \quad (23)$$

it is not the virtual photon probing the target but this $q\bar{q}$ state, and this is the basis of the shadowing phenomenon. Hence, the naïve impulse approximation picture that was applied in this work to the nucleon's virtual meson cloud is only applicable if the relevant distances are larger than the coherence length l . As the important meson loop momenta are of the order of $|\mathbf{k}| \approx 0.8 \text{ GeV}$, the significant distances between the nucleon and the

⁵In this conjecture we manifestly differ with Refs. [21,22].

mesons driving the convolution integrals are $\langle r_{MN} \rangle \approx 0.25$ fm, and the shadowing condition in Eq. (23) is already satisfied at $x \lesssim 0.2$. This underlines our conclusion that at small x , where absorptive effects are important, the meson cloud picture is not adequate and different degrees of freedom are dominant.

Note that in most low energy nuclear physics applications of the meson-exchange picture absorptive effects are included, either via explicit treatment or by means of simply neglecting the $\delta(\mathbf{r})$ -contribution in the respective pion-exchange potentials. Also, these absorption effects should lead to a modification of the t -dependence of the process $e + p \rightarrow X + n$ for small x , namely the cross section would not behave $\propto t$ at $t \rightarrow 0$ due to interference of the pion exchange and the pion-Pomeron cut. This effect is well known in strong interaction physics, for a review see Ref. [63].

V. CONCLUSIONS

In this work, we have updated the analysis of the Sullivan mechanism, i.e., the contribution of the nucleon's virtual meson cloud to the deep inelastic structure functions, by using various recent improved parton distribution functions fit to the host of inclusive, deep inelastic lepton and neutrino scattering data. We have taken into account contributions from the two lightest mesons, the π and the K , and, at various Q^2 , we have separately adjusted the form factors in the octet and decuplet channels and in the strange and non-strange sectors to the $SU(3)$ and $SU(2)$ flavor breaking components of the nucleon's antiquark sea and, simultaneously, to its strange quark content.

We find that we can only achieve a good description of the $SU(3)$ as well as the $SU(2)$ flavor asymmetry of the nucleon's antiquark sea if we allow the πNN and $\pi N\Delta$ vertices to differ significantly, and that, in order to be able to also describe the tail of the strange quark component, we have to use harder cut-offs in the kaonic sector. While the agreement of our calculations with the data-based parametrizations is satisfactory and scale independent for the flavor breaking share of the nucleon's antiquark distributions, the corresponding flavor

singlet component is quite poorly described in the convolution picture. This stresses the importance of gluonic degrees of freedom, even at such a low scale as $Q^2 = 1 \text{ GeV}^2$.

In particular, our analysis suggests exponential cut-off masses of $\Lambda_{\pi NN}^e \approx 1000 \text{ MeV}$, $\Lambda_{\pi N\Delta}^e \approx 800 \text{ MeV}$ and $\Lambda_{KNY}^e \approx 1200 \text{ MeV}$, respectively. These results are based on two recent empirical parton distribution functions, MRS(A') and CTEQ3M, which agree well with both the determination of the nucleon's strange quark content by the CCFR collaboration, related to the $SU(3)$ breaking, and the measurement of the $SU(2)$ asymmetry by the NA51 collaboration. Due to our inability to clearly distinguish between gluonic and meson cloud contributions in the flavor singlet channel, the $\Lambda_{\pi NN}^e$ and Λ_{KNY}^e given here are upper bounds of those quantities, while the $\Lambda_{\pi N\Delta}^e$ has to be understood as a lower limit.

Our findings are in qualitative agreement with the faster fall-off of the $p \rightarrow \Delta$ electromagnetic transition form factor as compared to the proton's electromagnetic form factor, and they suggest a sound breaking of the naïve $SU(6)$ symmetry relating the quark-substructure of the nucleon and the Δ -isobar. Also, the vertices that we obtain from our analysis of the deep inelastic scattering process are still significantly softer than those employed in most effective NN potentials fit to the rich body of experimental phase shift data, although the discrepancy we find is smaller than that quoted in early works in this context. They correspond to a typical quark confinement size of about 0.6 fm .

Note, however, that the meson loop momenta that are probed in the deep inelastic process investigated here, $|\mathbf{k}| \approx 0.8 \text{ GeV}$, are very different from those relevant for low-energy nuclear physics phenomena, as, for instance, in the meson-exchange descriptions of the NN interaction, and the respective distances are smaller than the typical confinement size. This indicates the limitations of applicability of the physical picture of a meson cloud around the nucleon.

ACKNOWLEDGMENTS

We wish to thank J.M. Eisenberg and M. Sargsyan for many useful discussions. This work

was supported in part by the Israel-USA Binational Science Foundation Grant No. 9200126, by the MINERVA Foundation of the Federal Republic of Germany, and by the U.S. Department of Energy under Contract No. DE-FG02-93ER40771.

REFERENCES

- [1] E.M.Henley, and G.A. Miller, Phys. Lett. **B251**, 453 (1990).
- [2] P. Amaudruz et al., Phys. Rev. Lett. **66**, 2712 (1991) and Phys. Rev. **D50**, R1 (1994).
- [3] R. Machleidt, K. Holinde, and Ch. Elster, Phys. Rep. **149**, 1 (1987).
- [4] B.A. Li, and K.F. Liu, *Chiral Solitons*, pp. 421, ed. K.F. Liu (World Scientific, 1987).
- [5] K.F. Liu, S.J. Dong, T. Draper, and W. Wilcox, Preprint UK/94-01 (1994).
- [6] T. Meissner, Preprint USC(NT)-95-4 (1995).
- [7] S. Coon, and M.D. Scadron, Phys. Rev. **C23**, 1150 (1981).
- [8] A. Thomas, and K. Holinde, Phys. Rev. Lett. **63**, 2025 (1989).
- [9] T.S.H. Lee, Argonne preprint ANL-PHY-7946-TH-95 (1995); T.S.H. Lee, Phys. Rev. Lett. **50**, 1571 (1983).
- [10] F. Güttner, G. Chanfray, H.J. Pirner, and B. Povh, Nucl. Phys. **A429**, 389 (1984).
- [11] H.-C. Kim, J.W. Durso, and K. Holinde, Phys. Rev. **C49**, 2353 (1994); C. Schütz, J.W. Durso, K. Holinde, and J. Speth, *ibid.* **C49**, 2671 (1994).
- [12] G. Janssen, J.W. Durso, K. Holinde, B.C. Pearce, and J. Speth, Phys. Rev. Lett. **71**, 1978 (1993).
- [13] J. Haidenbauer, K. Holinde, and A.W. Thomas, Phys. Rev. **C49**, 2331 (1994).
- [14] A. W. Thomas, Phys. Lett. **126B**, 97 (1983).
- [15] L.L. Frankfurt, L. Mankiewicz, and M.I. Strikman, Z. Phys. **A334**, 343 (1989).
- [16] S. Kumano, Phys. Rev. **D43**, 59 (1991); *ibid.* 3067.
- [17] A.I. Signal, A.W. Schreiber, and A.W. Thomas, Mod. Phys. Lett. **A6**, 271 (1991).
- [18] W. Melnitchouk, A.W. Thomas, and A.I. Signal, Z. Phys. **A340**, 85 (1991).

- [19] V.R. Zoller, Z. Phys. **C53**, 443 (1992).
- [20] C.M. Shakin, and W.-D. Sun, Phys. Rev. **C50**, 2553 (1994).
- [21] W.-Y.P. Hwang, J. Speth, and G.E. Brown, Z. Phys. **A340**, 383 (1991).
- [22] A. Szczurek, and J. Speth, Nucl. Phys. **A555**, 249 (1993).
- [23] W. Melnitchouk, and A.W. Thomas, Phys. Rev. **D47**, 3794 (1993).
- [24] A.D. Martin, W.J. Stirling, and R.G. Roberts, Preprint RAL-95-021 (1995).
- [25] H.L. Lai et al. (CTEQ Collaboration), Preprint MSU-HEP-41024 (1994).
- [26] J.D. Sullivan, Phys. Rev. **D5**, 1732 (1972).
- [27] B. Holzenkamp, K. Hollinde, and J. Speth, Nucl. Phys. **A500**, 485 (1989).
- [28] V. Stoks et al., Phys. Rev. **C47**, 512 (1993).
- [29] R.M. Davidson, and N.C. Mukhopadhyay, Phys. Rev. **D42**, 20 (1990); R.M. Davidson, N.C. Mukhopadhyay, and R. Wittman, Phys. Rev. **D43**, 71 (1991).
- [30] M. Buballa, Preprint SUNY-NTG-94-61 (1994).
- [31] S. Th  berge, G.A Miller, and A.W. Thomas, Can. J. Phys. **60**, 59 (1982).
- [32] M. Gl  ck, E. Reya, and A. Vogt, Preprint DESY 94-206 (1994).
- [33] E.L. Berger, and R. Meng, Phys. Lett. **B304**, 318 (1993).
- [34] A.D. Martin, W.J. Stirling, and R.G. Roberts, Phys. Lett. **B306**, 145 (1993).
- [35] M. Gl  ck, E. Reya, and A. Vogt, Z. Phys. **C53**, 651 (1992).
- [36] R. Kobayashi, M. Konuma and S. Kumano, Preprint SAGA-HE-63-94 (1994).
- [37] V.N. Gribov and L.N. Lipatov, Sov. J. Nucl. Phys. **15**, 438 and 675 (1972); L.N. Lipatov, Sov. J. Nucl. Phys. **20**, 94 (1974); G. Altarelli and G. Parisi, Nucl. Phys. **B126**, 298

- (1977); Yu.L. Dokshitzer, Sov. Phys. - JETP **46**, 641 (1977);
- [38] A.O. Bazarko et al. (CCFR Collaboration), Z. Phys. **C65**, 189 (1995).
- [39] A. Baldit et al. (NA51 Collaboration), Phys. Lett. **B332**, 244 (1994).
- [40] P.L. McGaughey et al. (CDF Collaboration), Phys. Rev. Lett. **69**, 1726 (1992).
- [41] P.J. Sutton, A.D. Martin, R.G. Roberts, and W.J. Stirling, Phys. Rev. **D45**, 2349 (1992).
- [42] M. Glück, E. Reya, and A. Vogt, Z. Phys. **C53**, 127 (1992).
- [43] J.G. Morfin, and W.K. Tung, Z. Phys. **C52**, 13 (1991).
- [44] P.N. Harriman, A.D. Martin, W.J. Stirling, and R.G. Roberts, Phys. Rev. **D42**, 798 (1990).
- [45] M. Diemoz, F. Ferroni, E. Longo, and G. Martinelli, Z. Phys. **C39**, 21 (1988).
- [46] E. Eichten, I. Hinchliffe, K. Lane, and C. Quigg, Rev. Mod. Phys. **56**, 579 (1984), and *ibid.* **58**, 1065 (1985).
- [47] J.F. Owen, Phys. Lett. **B266**, 126 (1991).
- [48] R.D. Field, and R.P. Feynman, Phys. Rev. **D15**, 2590 (1977).
- [49] A.D. Martin, W.J. Stirling, and R.G. Roberts, Phys. Rev. **D50**, 6734 (1994).
- [50] W. Struve, C. Hajduk, P.U. Sauer, and W. Theis, Nucl. Phys. **A465**, 651 (1987).
- [51] Th.A. Rijken, Ann. Phys. (N.Y.) **208**, 253 (1991).
- [52] L. Ray, C. Ordoñez, and U. van Kolck, Phys. Rev. Lett. **72**, 1982 (1994).
- [53] M.J. Musolf, and M. Burkhardt, Z. Phys. **C61**, 433 (1994).
- [54] CEBAF proposal No. PR-91-004, E.J. Beise spokesperson; CEBAF proposal No. PR-91-010, J.M. Finn and P.A. Souder spokespersons; CEBAF proposal No. PR-91-017,

D.H. Beck spokesperson.

- [55] P. Stoler, Phys. Rep. **226**, 103 (1993).
- [56] N. Isgur, and G. Karl, Phys. Rev. **D18**, 4187 (1978), and *ibid.* **D19**, 2653 (1979).
- [57] A. Chodos, R.L. Jaffe, K. Johnson, C.B. Thorn and V.F. Weisskopf, Phys. Rev. **D9**, 3471 (1974).
- [58] A.I. Signal and A.W. Thomas, Phys. Lett. **B211**, 481 (1988); A.I. Signal and A.W. Thomas, Phys. Rev. **D40**, 2832 (1989); A.W. Schreiber, A.I. Signal and A.W. Thomas, Phys. Rev. **D44**, 2653 (1991).
- [59] G.G. Simon et al., Nucl. Phys. **A333**, 381 (1980).
- [60] M. Strikman, *Proceedings of the XXVI International Conference on High Energy Physics, Vol. I*, Dallas, USA, 1992, AIP Conference Proceedings **272**, 806 (1992).
- [61] P. Amaudruz et al., Nucl. Phys. **B371**, 3 (1991).
- [62] G.T. Gravey et al., Fermilab proposal P866 (1992).
- [63] K.G. Boreskov, Sov. J. Nucl. Phys. **21**, 425 (1975) and *ibid.* **24**, 411 (1976).